

## $T$ -odd correlation in the $K_{l3\gamma}$ -decay

V.V. Braguta<sup>†</sup>, A.A. Likhoded<sup>††</sup>, A.E. Chalov<sup>†</sup>

<sup>†</sup> *Moscow Institute of Physics and Technology, Dolgoprudny, 141700 Russia*

<sup>††</sup> *Institute for High Energy Physics, Protvino, 142284 Russia*

*e-mail: andre@mx.ihep.su*

### Abstract

The dependence of the  $K^+ \rightarrow \pi^0 l^+ \nu_l \gamma$  decay width on the  $T$ -odd kinematical variable,  $\xi = \vec{q} \cdot [\vec{p}_l \times \vec{p}_\pi]/M^3$ , is studied at the tree and one-loop levels of Standard Model. It is shown that at the tree level this decay width is the even function of  $\xi$ , while the odd contribution arises due to the electromagnetic final state interaction. This contribution is determined by imaginary parts of one-loop diagrams. The calculations performed show that the  $\xi$ -odd contribution to the  $K^+ \rightarrow \pi^0 l^+ \nu_l \gamma$  and  $K^+ \rightarrow \pi^0 \mu^+ \nu_\mu \gamma$  decay widths is four orders of magnitude smaller than even contribution coming from the tree level of SM.

# Introduction

The study of rare radiative  $K$ -meson decays provide an interesting possibility to search for effects of a new physics beyond the Standard Model (SM). In particular, the search for new  $CP$ -violating interactions is of special interest. Contrary to SM, where the  $CP$ -violation is caused by the presence of the complex phase in the CKM matrix, the  $CP$ -violation in extended models can naturally arise due to the presence of, for instance, new charged Higgs bosons, which have complex couplings to fermions [1], hypothetical tensor interactions [2], etc.  $CP$ -violating effects can be probed with experimental observables, which are especially sensitive to  $T$ -odd contributions. Such observables are the rate dependence on  $T$ -odd correlation ( $\xi = \frac{1}{M_K^3} \vec{p}_\gamma \cdot [\vec{p}_\pi \times \vec{p}_l]$ ) in the  $K^\pm \rightarrow \pi^0 \mu^\pm \nu \gamma$  process [3] and transverse muon polarization in the  $K^\pm \rightarrow \mu^\pm \nu \gamma$  decays [4]. The experiments conducted thus far do not provide the sensitivity level, which is necessary to analyze the differential distributions in the  $K^\pm \rightarrow \pi^0 \mu^\pm (e^\pm) \nu \gamma$  decays. However, new perspectives are connected with the planned OKA experiment [5], where expected statistics of  $\sim 7.0 \cdot 10^5$  events for the  $K^+ \rightarrow \pi^0 \mu^+ \nu \gamma$  decay allows one to perform detailed analysis of the data and either probe new effects or put strict bounds on the parameters of extended models.

Searching for possible  $T$ -violating effects caused by new interactions in the  $K^+ \rightarrow \pi^0 \mu^+ \nu \gamma$  decays it is especially important to estimate the SM contribution to  $\xi$ -distribution, which is induced by electromagnetic final state interaction and which is natural background for new interaction contributions.

The Weinberg model with three Higgs doublets [1,6] is especially interesting for the search of possible  $T$ -violation. This model allows one to have complex Yukawa couplings that leads to extremely interesting phenomenology. It was shown [3] that the study of the  $T$ -odd correlation in the  $K^+ \rightarrow \pi^0 \mu^+ \nu \gamma$  process allows one either to probe the terms, which are linear in  $CP$ -violating couplings, or strictly confine the Weinberg model parameters.

In this paper, in the framework of SM we analyze the  $K^+ \rightarrow \pi^0 l^+ \nu_l \gamma$  decay width dependence on the kinematical variable  $\xi = \vec{q} \cdot [\vec{p}_l \times \vec{p}_\pi] / M^3$ . In general case, the width differential distribution,  $\rho(\xi) = d\Gamma/d\xi$ , can be represented as the sum of the even,  $f_{even}$ , and odd,  $f_{odd}$ , functions of  $\xi$ . At the tree level of SM the odd part,  $f_{odd}$ , does not contribute to the width distribution. We will show later that this effect is a direct consequence of the following fact: in the chiral perturbation theory the formfactors contributing to the matrix element do not have imaginary parts. However, the SM radiative corrections due to the electromagnetic final state interaction lead to the appearance of formfactors imaginary parts [7], that, in its turn, results in a nonvanishing  $\xi$ -odd contribution in the  $K^+ \rightarrow \pi^0 l^+ \nu_l \gamma$  decay width distribution. In this paper we analyze this effect at the one-loop level of SM. The matrix element of the  $K^+ \rightarrow \pi^0 l^+ \nu_l \gamma$  decay is calculated in the leading approximation of the chiral perturbation theory, i.e. up to the terms of  $O(p^4)$  [8].

To probe the  $T$ -odd effect we introduce, besides  $f_{odd}$ , the  $\xi$ -asymmetrical physical observable, which is defined as follows

$$A_\xi = \frac{N_+ - N_-}{N_+ + N_-}, \quad (1)$$

where  $N_+$  and  $N_-$  are the numbers of events with  $\xi > 0$  and  $\xi < 0$ , correspondingly.

One can see that while the  $A_\xi$  nominator depends on  $f_{odd}(\xi)$  only the denominator is proportional to  $f_{even}(\xi)$ , that makes this variable sensitive to  $\xi$ -odd effects.

As we will show later, the “background” SM one-loop contribution to  $f_{odd}$  is severely suppressed with respect to  $f_{even}$  ( $f_{odd}/f_{even} \sim 10^{-4}$ ). This allows us to state that proposed observables,  $A_\xi$  and  $f_{odd}$ , sensitive to  $T$ -odd contributions, provide good chance to search for the  $CP$ -violating effects beyond SM.

Another variable, sensitive to the  $CP$ -violation, is the transverse muon polarization,  $P_T$ , which can be observed in the  $K^+ \rightarrow \pi^0 \mu^+ \nu$  and  $K^+ \rightarrow \mu^+ \nu \gamma$  decays [4,7,9]. As in the case of  $\xi$ -dependence of the  $K^+ \rightarrow \pi^0 l^+ \nu_l \gamma$  rate, the presence of nonvanishing transverse polarization in SM is caused by the electromagnetic final state interaction. Though the  $P_T$  value is sensitive to  $T$ -odd effects, its measurement in the experiment seems to be cumbersome [10]. As for the  $A_\xi$  and  $f_{odd}$  variables, their experimental measurement is much more easier, that is one of the main advantages of these variables in comparison with the transverse muon polarization. The low event rate of the processes, where these values can be measured, is considered to be as the disadvantage of these variables. However, the anticipated statistics on the  $K^+ \rightarrow \pi^0 \mu^+ \nu \gamma$  process in the OKA experiment definitely allows one to use these observables to search for new  $CP$ -violating contributions.

In the first section we analyze the  $K^+ \rightarrow \pi^0 l^+ \nu_l \gamma$  decay width dependence on the  $T$ -odd correlation at the tree level of SM. In Section II we calculate SM contributions to the  $T$ -odd correlation, induced by one-loop diagrams. Last section contains the discussion and conclusions.

## 1 -odd correlation at the tree level of SM

The Feynman diagrams contributing to the  $K^+(p) \rightarrow \pi^0(p') l^+(p_l) \nu_l(p_\nu) \gamma(q)$  decay at the tree level of SM are shown in Fig 1. The tree-level amplitude for this process can be written as [8]:

$$T = \frac{G_F}{\sqrt{2}} e V_{us}^* \epsilon^\mu(q)^* \left( (V_{\mu\nu} - A_{\mu\nu}) \bar{u}(p_\nu) \gamma^\nu (1 - \gamma_5) v(p_l) + \frac{F_\nu}{2p_l q} \bar{u}(p_\nu) \gamma^\nu (1 - \gamma_5) (m_l - \hat{p}_l - \hat{q}) \gamma_\mu v(p_l) \right), \quad (2)$$

where

$$V_{\mu\nu} = i \int d^4x e^{iqx} \langle \pi^0(p') | T V_\mu^{em}(x) V_\nu^{4-i5}(0) | K^+(p) \rangle \quad (3)$$

$$A_{\mu\nu} = i \int d^4x e^{iqx} \langle \pi^0(p') | T V_\mu^{em}(x) A_\nu^{4-i5}(0) | K^+(p) \rangle, \quad (4)$$

and  $F_\nu$  is the matrix element of the  $K_{l3}^+$ -decay:

$$F_\nu = \langle \pi^0(p') | V_\nu^{4-i5}(0) | K^+(p) \rangle. \quad (5)$$

Here  $p'$ ,  $p_l$ ,  $q$ ,  $p_\nu$ ,  $p$  are the pion, lepton,  $\gamma$ -quantum, neutrino, and kaon four-momenta, correspondingly. In the leading approximation of the chiral perturbation theory  $A_{\mu\nu} = 0$

and expressions for  $V_{\mu\nu}$  and  $F_\mu$  can be written as

$$\begin{aligned}
F_\mu &= \frac{1}{\sqrt{2}}(p + p')_\mu \\
V_{\mu\nu} &= V_1(g_{\mu\nu} - \frac{W_\mu q_\nu}{qW}) + V_2(p'_\mu q_\nu - \frac{p'q}{qW}W_\mu q_\nu) + \frac{p_\mu}{pq}F_\nu \\
W_\mu &= (p_l + p_\nu)_\mu \\
V_1 &= \frac{1}{\sqrt{2}}, \quad V_2 = -\frac{1}{\sqrt{2}pq}.
\end{aligned}$$

So, the matrix element of the decay can be rewritten in the following form:

$$\begin{aligned}
T &= \frac{G_F}{2} e V_{us}^* \epsilon^\mu(q)^* \cdot \bar{u}(p_\nu)(1 + \gamma_5) \cdot \\
&\quad \left( (\hat{p} + \hat{p}') \left( \frac{p_\mu}{(pq)} - \frac{(p_l)_\mu}{(p_l q)} \right) - (\hat{p} + \hat{p}') \frac{\hat{q}\gamma_\mu}{2(p_l q)} + \left( \gamma_\mu - \frac{\hat{q}p_\mu}{(pq)} \right) \right) u(p_l), \quad (6)
\end{aligned}$$

and the  $K^+ \rightarrow \pi^0 l^+ \nu \gamma$  decay partial width can be calculated by integrating over the phase space.

In Fig. 2 we present the differential distribution of the decay partial width in the  $K$ -meson rest frame over the three-momenta of final particles and the angle between the lepton and  $\gamma$ -quantum directions, calculated at the tree level of SM. For the case of the electron channel (see Fig. 2a) the bulk of the width value is collected in the region of small values of the lepton and  $\gamma$ -quantum momenta, maximal values of the pion momenta, and small angles between lepton and  $\gamma$ -quantum momenta.

In the case of the muon channel (see Fig. 2b) the bulk of the width is collected in the region of intermediate values of lepton momentum, small values of the  $\gamma$ -quantum momentum, maximal values of the pion momentum, and small angles between the lepton and  $\gamma$ -quantum directions.

Imposing the kinematical cuts on the  $\gamma$ -quantum energy and lepton- $\gamma$ -quantum scattering angle in the kaon rest frame,  $E_\gamma > 30$  MeV and  $\theta_{\gamma l} > 20^\circ$ , which are typical for the current and planned kaon experiments, one gets the following branching values:

$$\begin{aligned}
\text{Br}(K^+ \rightarrow \pi e^+ \nu_e \gamma) &= 3.18 \cdot 10^{-4}, \\
\text{Br}(K^+ \rightarrow \pi \mu^+ \nu_\mu \gamma) &= 2.15 \cdot 10^{-5},
\end{aligned}$$

which are in a good agreement with earlier calculations (see, for instance, [8]) and existing experimental results [11].

Looking for possible  $CP$ -odd contributions we will investigate the decay width distribution over variable  $\xi = \vec{q} \cdot [\vec{p}_l \times \vec{p}_\pi] / M^3$ , which changes the sign under  $CP$ - or  $T$ -conjugation,

$$\rho(\xi) = \frac{d\Gamma}{d\xi}, \quad (7)$$

This distribution is an ‘‘indicator’’ for the  $T$ -violation effects. The  $\rho(\xi)$  function can be rewritten as

$$\rho = f_{\text{even}}(\xi) + f_{\text{odd}}(\xi),$$

where  $f_{even}(\xi)$  and  $f_{odd}(\xi)$  are the even and odd functions of  $\xi$ , correspondingly. The function  $f_{odd}(\xi)$  can be represented as follows

$$f_{odd} = g(\xi^2)\xi . \quad (8)$$

It is evident, that after integration of the  $\rho(\xi)$  function over whole region of  $\xi$  only the  $f_{even}(\xi)$  function contributes to the total width. In Fig. 3 we present the  $\rho(\xi)/\Gamma_{total}$  distributions for the  $K^+ \rightarrow \pi^0\mu^+\nu_l\gamma$  and  $K^+ \rightarrow \pi^0e^+\nu_l\gamma$  decays. Indeed, one can see from Fig. 3 that at the tree level of SM, where there are no any  $T$ -odd contributions, the distributions, as one could expect, are strictly symmetric with respect to the line  $\xi = 0$ , i.e. the numbers of events of the  $K^+ \rightarrow \pi^0l^+\nu_l\gamma$  decay with  $\xi > 0$  and  $\xi < 0$  are equal. This fact can be explained by following: in the case of the tree approximation of SM the matrix element squared is expressed via scalar products of final particles momenta only, and, consequently, there are no contributions linear over  $\xi$ . So, the  $\rho(\xi)$  function is essentially even function of  $\xi$ .

Analysing the  $K^+ \rightarrow \pi^0l^+\nu_l\gamma$  data, it is useful to introduce, besides the  $\rho(\xi)$  distribution, the integral asymmetry, which is defined as

$$A_\xi = \frac{N_+ - N_-}{N_+ + N_-} , \quad (9)$$

where  $N_+$  and  $N_-$  are the numbers of decay events with  $\xi > 0$  and  $\xi < 0$ . It is easy to see that the  $A_\xi$  nominator depends on  $f_{odd}(\xi)$  only, which makes this variable highly sensitive to  $T$ -odd effects beyond SM.

## 2 -odd correlation in SM due to the final state interaction

Nonvanishing value of the  $A_\xi$ -asymmetry as well as odd contribution to  $\rho(\xi)$  can arise in SM due to the electromagnetic final state interaction at the level of one-loop diagrams. The most general expression for the  $K^+ \rightarrow \pi^0l^+\nu_l\gamma$  decay amplitude with account for the electromagnetic radiative corrections (implying the gauge invariance) can be written as follows:

$$\begin{aligned} T_{one-loop} = & \frac{G_F}{\sqrt{2}} e V_{us}^* \epsilon_\nu^* \bar{u}(p_\nu) (1 + \gamma_5) \cdot \\ & \cdot \left( C_1(p^\nu - \frac{pq}{p_l q} p_l^\nu) + C_3((p')^\nu - \frac{p'q}{p_l q} p_l^\nu) + C_5(p^\nu - \frac{pq}{p_l q} p_l^\nu) \hat{p}' \right. \\ & + C_7((p')^\nu - \frac{p'q}{p_l q} p_l^\nu) \hat{p}' + C_9(\hat{q} p^\nu - (pq)\gamma^\nu) \\ & + C_{10}(\hat{q} p_l^\nu - (p_l q)\gamma^\nu) + C_{11}(\hat{q}(p')^\nu - (p'q)\gamma^\nu) + C_{12}\hat{q}\gamma^\nu \\ & + C_{13}\hat{p}'(\hat{q} p^\nu - (pq)\gamma^\nu) + C_{14}\hat{p}'(\hat{q} p_l^\nu - (p_l q)\gamma^\nu) \\ & \left. + C_{15}\hat{p}'(\hat{q}(p')^\nu - (p'q)\gamma^\nu) + C_{16}\hat{p}'\hat{q}\gamma^\nu \right) v(p_l) , \quad (10) \end{aligned}$$

Where the  $C_i$  coefficients are the kinematical factors, which are due to one-loop diagram contributions. The matrix element squared with account for the one-loop contributions can be rewritten in the following form:

$$|T_{one-loop}|^2 = |T_{even}|^2 + |T_{odd}|^2, \quad (11)$$

where

$$\begin{aligned}
|T_{odd}|^2 = & -2G_F^2 e^2 |V_{us}|^2 m_K^4 \xi \left( \text{Im}(C_1) m_l \left( 2 \frac{1}{p_l q} - 4 \frac{pq}{(p_l q)^2} \right) \right. \\
& - \text{Im}(C_3) m_l \left( 2 \frac{1}{p_l q} + 4 \frac{p'q}{(p_l q)^2} \right) \\
& + \text{Im}(C_5) \left( 4 + 2m_l^2 \frac{pq}{(p_l q)^2} + \frac{1}{p_l q} (2m_K^2 - 2m_\pi^2 + 4pp' \right. \\
& \left. - 4pp_l - 4pq - 4p'l_l - 4p'q) \right) \\
& + \text{Im}(C_7) \left( 2m_l^2 \frac{p'q}{(p_l q)^2} + 4 \frac{m_\pi^2}{p_l q} \right) + \text{Im}(C_9) \left( 8 \frac{pp_l}{p_l q} - 8 \frac{m_K^2}{pq} \right) \\
& + \text{Im}(C_{10}) \left( 8 \frac{m_l^2}{p_l q} + 8 \frac{p_l q}{pq} - 8 \frac{pp_l}{pq} - 8 \right) + \text{Im}(C_{11}) \left( 8 \frac{p'q}{pq} + 8 \frac{p'l_l}{p_l q} - 8 \frac{pp'}{pq} \right) \\
& + \text{Im}(C_{12}) \left( 4 \frac{m_l}{pq} - 8 \frac{m_l}{p_l q} \right) + \text{Im}(C_{13}) m_l \left( 4 \frac{m_K^2}{pq} - 4 \frac{pp_l}{p_l q} \right) \\
& + \text{Im}(C_{14}) m_l \left( 4 + 4 \frac{pp_l}{pq} - 4 \frac{m_l^2}{p_l q} - 4 \frac{p_l q}{pq} \right) \\
& + \text{Im}(C_{15}) m_l \left( 4 \frac{pp'}{pq} - 4 \frac{p'q}{pq} - 4 \frac{p'l_l}{p_l q} \right) \\
& + \text{Im}(C_{16}) \left( -8 + 4 \frac{m_K^2}{pq} - 4 \frac{m_\pi^2}{pq} + 8 \frac{pp'}{pq} \right. \\
& \left. - 8 \frac{pp_l}{pq} - 8 \frac{p'l_l}{pq} - 8 \frac{p'q}{pq} + 4 \frac{m_l^2}{p_l q} + 8 \frac{p_l q}{pq} \right) \quad (12)
\end{aligned}$$

As one can see from Eqs. (11) and (12), the nonvanishing contribution to  $f_{odd}(\xi)$  and  $A_\xi$  (linear over  $\xi$ ) is determined by the one-loop electromagnetic corrections, which lead to the appearance of imaginary parts of the  $C_i$  formfactors.

To calculate the formfactor imaginary parts one can use the  $S$ -matrix unitarity [7]:

$$S^\dagger S = 1.$$

Using  $S = 1 + iM$ , one gets

$$M_{fi} - M_{if}^* = i \sum_n M_{nf}^* M_{ni}, \quad (13)$$

where  $i, f, n$  indices correspond to the initial, final, and intermediate states of the particle system. Further, using the  $T$ -invariance of the matrix element one has

$$\begin{aligned}
\text{Im} M_{fi} &= \frac{1}{2} \sum_n M_{nf}^* M_{ni} \\
M_{fi} &= (2\pi)^4 \delta(P_f - P_i) T_{fi}
\end{aligned}$$

one-loop diagrams, which describe the electromagnetic corrections to the  $K^+ \rightarrow \pi l^+ \nu_l \gamma$  process and lead to imaginary parts of the formfactors in (10), thus contributing to  $f_{odd}(\xi)$ , are shown in Fig. 3. Using Eq. (2) one can write down the imaginary parts of these diagrams, which give the nonvanishing contribution to  $f_{odd}(\xi)$ . It is useful to split the whole set of one-loop diagrams in to two groups. The first group contains the diagrams shown in Figs. 4a, 4c, 4e. The imaginary part of these diagrams can be written as follows:

$$\begin{aligned} \text{Im}T_1 = \frac{\alpha}{2\pi} \frac{G_F}{\sqrt{2}} e V_{us}^* \bar{u}(p_\nu) (1 + \gamma_5) \int \frac{d^3 k_\gamma}{2\omega_\gamma} \frac{d^3 k_l}{2\omega_l} \delta(k_\gamma + k_l - q - p_l) \cdot \\ \cdot \hat{R}_\mu(\hat{k}_l - m_l) \gamma^\mu \frac{\hat{q} + \hat{p}_l - m_l}{(q + p_l)^2 - m_l^2} \gamma^\delta \varepsilon_\delta^* v(p_l) \end{aligned} \quad (14)$$

The second group includes the diagrams shown in Figs. 4b, 4d, 4f. The corresponding imaginary part is

$$\begin{aligned} \text{Im}T_2 = \frac{\alpha}{2\pi} \frac{G_F}{\sqrt{2}} e V_{us}^* \bar{u}(p_\nu) (1 + \gamma_5) \int \frac{d^3 k_\gamma}{2\omega_\gamma} \frac{d^3 k_l}{2\omega_l} \delta(k_\gamma + k_l - q - p_l) \cdot \\ \cdot \hat{R}_\mu(\hat{k}_l - m_l) \gamma^\delta \varepsilon_\delta^* \frac{\hat{k}_\mu - \hat{q} - m_l}{(k_\mu - q)^2 - m_l^2} \gamma^\mu v(p_l), \end{aligned} \quad (15)$$

where

$$\hat{R}_\mu = (V_{\mu\nu} - A_{\mu\nu}) \gamma^\nu - \frac{F_\nu}{2p_l q} \gamma^\nu (\hat{p}_l + \hat{q} - m_l) \gamma_\mu \quad (16)$$

The details of the integrals calculation entering Eqs. (14), (15), and their dependence on kinematical parameters are given in Appendix 1. Expressions for imaginary parts of the  $C_i$  formfactors are given in Appendix 2.

### 3 Results and discussions

Before discussing the numerical results, let us note that considering one-loop diagrams we neglected their contributions to the even part of the  $\xi$ -distribution, as these contributions are considerably smaller than nonzero contribution to  $f_{even}$  from the tree approximation of SM. However, in the case of  $f_{odd}$  the tree SM contribution is equal to zero, thus the contributions to  $f_{odd}$  coming from one-loop diagrams become essential. Analysing the  $K^+ \rightarrow \pi^0 l^+ \nu_l \gamma$  width dependence on the kinematical variable  $\xi$  we separately consider two decay channels,  $K^+ \rightarrow \pi^0 e^+ \nu_e \gamma$  and  $K^+ \rightarrow \pi^0 \mu^+ \nu_\mu \gamma$ , since the functional  $\xi$ -dependence of the width in these two case is essentially different.

$$\underline{K^+ \rightarrow \pi^0 e^+ \nu_e \gamma}$$

In Fig. 5a we show the  $\xi$ -odd contribution to the differential width distribution, which is induced by the imaginary parts of one-loop diagrams shown in Fig. 3. In the kinematical region of the  $\xi$  parameter the value of the width distribution varies in the interval of  $(-2.0 \div 2.0) \cdot 10^{-6}$ , and the sign of  $f_{odd}$  is opposite to the sign of  $\xi$ . As the total  $\xi$ -distribution is the sum of the even and odd parts, it leads to the fact that in experiment

one will observe the surplus of the events with negative  $\xi$  values. The asymmetry value for this channel is

$$A_\xi(K^+ \rightarrow \pi e^+ \nu_e \gamma) = -0.59 \cdot 10^{-4} .$$

$$\underline{K^+ \rightarrow \pi^0 \mu^+ \nu_\mu \gamma}$$

In Fig. 5b we present the  $\xi$ -odd contribution to the differential width distribution for the muon decay channel. The characteristic variation interval for this distribution is  $(-4.0 \div 4.0) \cdot 10^{-7}$ , but the sign of  $f_{odd}$  coincides with the sign of  $\xi$ . This results in the surplus of the events with positive  $\xi$  values. The asymmetry value for this channel is

$$A_\xi(K^+ \rightarrow \pi \mu^+ \nu_\mu \gamma) = 1.14 \cdot 10^{-4} .$$

This difference between the  $f_{odd}$  behaviour in cases of electron and muon channels can be explained as follows: for the muon decay channel the contributions from imaginary parts of the  $C_1$ ,  $C_{12}$ ,  $C_{13}$ , and  $C_{14}$  formfactors become essential, while in the case of the electron channel their contributions are negligible (these contributions are proportional to mass of the lepton).

It should be noted that the difference in the  $f_{odd}$  behaviour for the electron and muon channels could be used to disentangle the SM radiative and new physics contributions: in extended models, where the  $CP$ -violation can arise at tree level, the sign of the  $\xi$ -dependence is insensitive to the lepton flavor, as it takes place, for instance, in the Weinberg model [1].

We would like to underline that for the both decay channels the  $f_{odd}$  value is four orders of magnitude smaller than the tree contribution of SM. It allows to state that  $\xi$ -odd effects are severely suppressed in SM. Thus, the “background” SM contribution to the odd part of the  $\xi$ -dependence leaves the “window” to discover new  $CP$ -violating effects in these decays up to the level of  $10^{-4}$ .

Analysing the situation with the integral asymmetry  $A_\xi$  one sees that for reliable observation of  $\xi$ -odd effects from the asymmetry only one should have the data sample for these decays at least at the level of  $10^8$  events. In this respect the analysis of differential  $\xi$ -distribution seems to be very important.

## Acknowledgements

The authors would like to thank L.B. Okun for the critical remarks and interest to this calculations. The authors would like to acknowledge useful discussions and valuable remarks by V.A. Rubakov, A.K. Likhoded, and V.F. Obraztsov. This work was supported, in part, by the RFBR, grants 99-02-16558 and 00-15-96645, and RF Ministry of Education, grant 00-3.3-62.

# References

1. S. Weinberg, Phys. Rev. Lett. **37**, 651 (1976).
2. R.J. Tesarek, hep-ex/9903069.
3. A. Likhoded, V. Braguta, and A. Chalov, in press (see also, hep-ex/0011033).
4. A. Likhoded, V. Braguta, and A. Chalov, hep-ph/0105111.
5. V.F. Obraztsov, Nucl. Phys. B (Proc. Suppl.) **99**, 257 (2001).
6. J.F. Donoghue and B. Holstein, Phys. Lett. B **113**, 382 (1982); L. Wolfenstein, Phys. Rev. **29**, 2130 (1984); G. Barenboim et al., Phys. Rev. D **55**, 24213 (1997); M. Kobayashi, T.-T. Lin, and Y. Okada, Prog. Theor. Phys. **95**, 361 (1996); S.S. Gershtein et al., Z. Phys. C **24**, 305 (1984); R. Garisto and G. Kane, Phys. Rev. D **44**, 2038 (1991); G. Belanger and C.Q. Cheng, Phys. Rev. D **44**, 2789 (1991).
7. L.B. Okun and I.B. Khriplovich, Sov. Journ, Nucl. Phys. **6** , 821 (1967).
8. J. Bijnens, G. Ecker, and J. Gasser, Nucl. Phys. B **396**, 81 (1993).
9. A.R. Zhitnitskii, Sov. J. Nucl. Phys. **31**, 529 (1980); . , C.Q. Geng and J.N. Ng, Phys. Rev. D **42**, 1509 (1990); C.H. Chen, C.Q. Geng, and C.C. Lih, hep-ph/9709447; G. Hiller and G. Isidori, Phys. Lett. B **459**, 295 (1999).
10. See, for instance, Yu.G. Kudenko, hep-ex/00103007.
11. Review of Particle Physics, Euro. Phys. Journ. C **15**, 501 (2000).

# Appendix 1

Calculating the integrals, which contribute to Eqs. (14) and (15), we use the following notations:

$$P = p_l + q$$

$$d\rho = \frac{d^3 k_\gamma}{2\omega_\gamma} \frac{d^3 k_l}{2\omega_l} \delta(k_\gamma + k_l - P)$$

We present below either the explicit expressions for integrals, or the set of equations, which being solved, give the parameters, entering the integrals.

$$J_{11} = \int d\rho = \frac{\pi}{2} \frac{P^2 - m_l^2}{P^2},$$

$$J_{12} = \int d\rho \frac{1}{(pk_\gamma)} = \frac{\pi}{2I} \ln\left(\frac{(Pp) + I}{(Pp) - I}\right),$$

where

$$I^2 = (Pp)^2 - m_K^2 P^2.$$

$$\int d\rho \frac{k_\gamma^\alpha}{(pk_\gamma)} = a_{11} p^\alpha + b_{11} P^\alpha.$$

The  $a_{11}$  and  $b_{11}$  parameters are defined as follows

$$a_{11} = -\frac{1}{(Pp)^2 - m_K^2 P^2} \left( P^2 J_{11} - \frac{J_{12}}{2} (Pp)(P^2 - m_l^2) \right),$$

$$b_{11} = \frac{1}{(Pp)^2 - m_K^2 P^2} \left( (Pp) J_{11} - \frac{J_{12}}{2} m_K^2 (P^2 - m_l^2) \right)$$

$$\int d\rho k_\gamma^\alpha = a_{12} P^\alpha,$$

where

$$a_{12} = \frac{(P^2 - m_l^2)}{2P^2} J_{11},$$

$$J_1 = \int d\rho \frac{1}{(pk_\gamma)((p_l - k_\gamma)^2 - m_l^2)} = -\frac{\pi}{2I_1(P^2 - m_l^2)} \ln\left(\frac{(pp_l) + I_1}{(pp_l) - I_1}\right),$$

$$J_2 = \int d\rho \frac{1}{(p_l - k_\gamma)^2 - m_l^2} = -\frac{\pi}{4I_2} \ln\left(\frac{(Pp_l) + I_2}{(Pp_l) - I_2}\right),$$

where

$$I_1^2 = (pp_l)^2 - m_l^2 m_K^2,$$

$$I_2^2 = (Pp_l)^2 - m_l^2 P^2.$$

$$\begin{aligned}
\int d\rho \frac{k_\gamma^\alpha}{(p_l - k_\gamma)^2 - m_l^2} &= a_1 P^\alpha + b_1 p_l^\alpha, \\
a_1 &= -\frac{m_l^2(P^2 - m_l^2)J_2 + (Pp_l)J_{11}}{2((Pp_l)^2 - m_l^2 P^2)}, \\
b_1 &= \frac{(Pp_l)(P^2 - m_l^2)J_2 + P^2 J_{11}}{2((Pp_l)^2 - m_l^2 P^2)},
\end{aligned}$$

The integrals below are expressed in terms of the parameters, which can be obtained by solving the sets of equations.

$$\begin{aligned}
\int d\rho \frac{k_\gamma^\alpha}{(pk_\gamma)((p_l - k_\gamma)^2 - m_l^2)} &= a_2 P^\alpha + b_2 p^\alpha + c_2 p_l^\alpha, \\
\begin{cases} a_2(Pp) + b_2 m_K^2 + c_2(pp_l) = J_2 \\ a_2(Pp_l) + b_2(pp_l) + c_2 m_l^2 = -\frac{1}{2}J_{12} \\ a_2 P^2 + b_2(Pp) + c_2(Pp_l) = (p_l q)J_1 \end{cases}
\end{aligned}$$

$$\begin{aligned}
\int d\rho \frac{k_\gamma^\alpha k_\gamma^\beta}{(pk_\gamma)((p_l - k_\gamma)^2 - m_l^2)} &= a_3 g^{\alpha\beta} + b_3(P^\alpha p^\beta + P^\beta p^\alpha) + c_3(P^\alpha p_l^\beta + P^\beta p_l^\alpha) \\
&+ d_3(p^\alpha p_l^\beta + p^\beta p_l^\alpha) + e_3 p_l^\alpha p_l^\beta \\
&+ f_3 P^\alpha P^\beta + g_3 p^\alpha p^\beta,
\end{aligned}$$

$$\begin{cases} 4a_3 + 2b_3(Pp) + 2c_3(Pp_l) + 2d_3(pp_l) + g_3 m_K^2 + e_3 m_l^2 + f_3 P^2 = 0 \\ c_3(pp_l) + b_3 m_K^2 + f_3(Pp) - a_1 = 0 \\ c_3(Pp) + d_3 m_K^2 + e_3(pp_l) - b_1 = 0 \\ a_3 + b_3(Pp) + d_3(pp_l) + g_3 m_K^2 = 0 \\ b_3(pp_l) + c_3 m_l^2 + f_3(Pp_l) = -\frac{1}{2}b_{11} \\ b_3(Pp_l) + d_3 m_l^2 + g_3(pp_l) = -\frac{1}{2}a_{11} \\ a_3 P^2 + 2b_3 P^2(Pp) + 2c_3 P^2(Pp_l) + 2d_3(Pp_l)(Pp) + \\ \quad + e_3(Pp_l)^2 + f_3(P^2)^2 + g_3(Pp)^2 = (p_l q)^2 J_1 \end{cases}$$

$$\begin{aligned}
\int d\rho \frac{k_\gamma^\alpha k_\gamma^\beta}{(p_l - k_\gamma)^2 - m_l^2} &= a_4 g_{\alpha\beta} + b_4(P^\alpha p_l^\beta + P^\beta p_l^\alpha) + c_4 P^\alpha P^\beta + d_4 p_l^\alpha p_l^\beta, \\
\begin{cases} a_4 + d_4 m_l^2 + b_4(Pp_l) = 0 \\ b_4 m_l^2 + c_4(Pp_l) = -\frac{1}{2}a_{12} \\ 4a_4 + 2b_4(Pp_l) + c_4 P^2 + d_4 m_l^2 = 0 \\ a_4 P^2 + 2b_4 P^2(Pp_l) + c_4(P^2)^2 + d_4(Pp_l)^2 = \frac{(P^2 - m_l^2)^2}{4} J_2 \end{cases}
\end{aligned}$$

## Appendix 2

Here we present the explicit expressions for imaginary parts of the  $C_i$  formfactors via the parameters, calculated in Appendix 1.

$$\begin{aligned}
C_1 &= \frac{\alpha}{\sqrt{2\pi}} m_l (4a_3 + b_3 m_K^2 + d_3 m_K^2 - 2a_2 m_l^2 + 2b_3 m_l^2 - 2c_2 m_l^2 + 6c_3 m_l^2 \\
&\quad + 2d_3 m_l^2 + 3e_3 m_l^2 + 3f_3 m_l^2 - b_3 m_\pi^2 - d_3 m_\pi^2 - 2b_3(p'p_l) \\
&\quad - 2d_3(p'p_l) - 2b_3(p'q) - 2d_3(p'q) - 4a_2(p_lq) + 4b_3(p_lq) - 2c_2(p_lq) \\
&\quad + 8c_3(p_lq) + 2d_3(p_lq) + 2e_3(p_lq) + 6f_3(p_lq) + 2b_3(pp') + 2d_3(pp'))
\end{aligned}$$

$$\begin{aligned}
C_5 &= -\frac{\alpha}{\sqrt{2\pi}} (4a_3 - 4a_2 m_l^2 + 3b_3 m_l^2 - 4c_2 m_l^2 + 4c_3 m_l^2 + 3d_3 m_l^2 \\
&\quad + 2e_3 m_l^2 + 2f_3 m_l^2 - 4a_2(p_lq) + 4b_3(p_lq) + 4c_3(p_lq) + 4f_3(p_lq))
\end{aligned}$$

$$\begin{aligned}
C_9 &= -\frac{\alpha}{\sqrt{2\pi}} (2a_3 + b_3 m_K^2 - a_2 m_l^2 + b_3 m_l^2 - c_2 m_l^2 + 2c_3 m_l^2 \\
&\quad + d_3 m_l^2 + 2f_3 m_l^2 - b_3 m_\pi^2 - 2b_3(p'p_l) - 2b_3(p'q) - 2a_2(p_lq) \\
&\quad + 2b_3(p_lq) + 2c_3(p_lq) + 4f_3(p_lq) + 2b_3(pp'))
\end{aligned}$$

$$\begin{aligned}
C_{10} &= \frac{\alpha}{\sqrt{2\pi}} \frac{1}{(p_lq)} (-a_1 m_l^2 - b_1 m_l^2 + 2b_4 m_l^2 + c_4 m_l^2 + d_4 m_l^2 + 2a_3(p_lq) \\
&\quad + a_2 m_K^2(p_lq) - c_3 m_K^2(p_lq) - f_3 m_K^2(p_lq) - e_3 m_l^2(p_lq) \\
&\quad + f_3 m_l^2(p_lq) - a_2 m_\pi^2(p_lq) + c_3 m_\pi^2(p_lq) + f_3 m_\pi^2(p_lq) \\
&\quad - 2a_2(p'p_l)(p_lq) + 2c_3(p'p_l)(p_lq) + 2f_3(p'p_l)(p_lq) - 2a_2(p'q)(p_lq) \\
&\quad + 2c_3(p'q)(p_lq) + 2f_3(p'q)(p_lq) + 2f_3(p_lq)^2 + 2a_2(p_lq)(pp') \\
&\quad - 2c_3(p_lq)(pp') - 2f_3(p_lq)(pp') - 2a_2(p_lq)(ppi) + 2b_3(p_lq)(ppi) \\
&\quad + 2c_3(p_lq)(ppi) + 2f_3(p_lq)(ppi) - 2a_2(p_lq)(pq) + 2b_3(p_lq)(pq) \\
&\quad + 2c_3(p_lq)(pq) + 2f_3(p_lq)(pq))
\end{aligned}$$

$$\begin{aligned}
C_{12} &= -\frac{\alpha}{4\sqrt{2\pi}} \frac{m_l}{(p_lq)^2} (-2a_{12} m_l^2 - 2J_{11} m_l^2 - 2a_{12}(p_lq) \\
&\quad - 4a_4(p_lq) + 2J_{11}(p_lq) - a_{11} m_K^2(p_lq) + b_{11} m_K^2(p_lq) \\
&\quad + 8a_1 m_l^2(p_lq) + 8b_1 m_l^2(p_lq) - 4b_4 m_l^2(p_lq) - 2c_4 m_l^2(p_lq) \\
&\quad - 2d_4 m_l^2(p_lq) - 4J_2 m_l^2(p_lq) - b_{11} m_\pi^2(p_lq) - 2b_{11}(p'p_l)(p_lq) \\
&\quad - 2b_{11}(p'q)(p_lq) + 8a_1(p_lq)^2 + 4a_3(p_lq)^2 + 4b_1(p_lq)^2 - 4b_4(p_lq)^2 \\
&\quad - 4c_4(p_lq)^2 - 4J_2(p_lq)^2 + 2a_2 m_K^2(p_lq)^2 - 2b_2 m_K^2(p_lq)^2 \\
&\quad + 2c_2 m_K^2(p_lq)^2 + 2g_3 m_K^2(p_lq)^2 + 8c_3 m_l^2(p_lq)^2 + 6e_3 m_l^2(p_lq)^2 \\
&\quad + 2f_3 m_l^2(p_lq)^2 - 2a_2 m_\pi^2(p_lq)^2 - 2c_2 m_\pi^2(p_lq)^2 - 4a_2(p'p_l)(p_lq)^2)
\end{aligned}$$

$$\begin{aligned}
& -4c_2(p'l)(p_lq)^2 - 4a_2(p'q)(p_lq)^2 - 4c_2(p'q)(p_lq)^2 + 12c_3(p_lq)^3 \\
& + 4e_3(p_lq)^3 + 4f_3(p_lq)^3 + 2b_{11}(p_lq)(pp') + 4a_2(p_lq)^2(pp') \\
& + 4c_2(p_lq)^2(pp') - 2a_{11}(p_lq)(ppi) - 4b_{11}(p_lq)(ppi) + 2J_{12}(p_lq)(ppi) \\
& - 8a_2(p_lq)^2(ppi) - 4b_2(p_lq)^2(ppi) + 4b_3(p_lq)^2(ppi) - 8c_2(p_lq)^2(ppi) \\
& + 8d_3(p_lq)^2(ppi) + 4J_1(p_lq)^2(ppi) - 2a_{11}(p_lq)(pq) - 4b_{11}(p_lq)(pq) \\
& + 2J_{12}(p_lq)(pq) - 4a_2(p_lq)^2(pq) + 4b_3(p_lq)^2(pq) - 4c_2(p_lq)^2(pq) \\
& + 4d_3(p_lq)^2(pq)
\end{aligned}$$

$$C_{13} = -\frac{\alpha}{\sqrt{2\pi}}m_l(2a_2 - b_3 + 2c_2 - 2d_3)$$

$$\begin{aligned}
C_{14} &= \frac{\alpha}{\sqrt{2\pi}}\frac{m_l}{(p_lq)}(2a_1 + 2b_1 - 4b_4 - 2c_4 - 2d_4 + a_2(p_lq) + 3c_3(p_lq) \\
& + 2e_3(p_lq) + f_3(p_lq))
\end{aligned}$$

$$\begin{aligned}
C_{16} &= \frac{\alpha}{4\sqrt{2\pi}}\frac{1}{(p_lq)^2}(-4a_{12}m_l^2 - 4J_{11}m_l^2 - 4a_{12}(p_lq) - 8a_4(p_lq) + 4J_{11}(p_lq) \\
& - 2a_{11}m_K^2(p_lq) + 16a_1m_l^2(p_lq) + 16b_1m_l^2(p_lq) + b_{11}m_l^2(p_lq) \\
& - 8b_4m_l^2(p_lq) - 4c_4m_l^2(p_lq) - 4d_4m_l^2(p_lq) - 8J_2m_l^2(p_lq) \\
& + 16a_1(p_lq)^2 + 4a_3(p_lq)^2 + 8b_1(p_lq)^2 - 8b_4(p_lq)^2 - 8c_4(p_lq)^2 \\
& - 2J_{12}(p_lq)^2 - 8J_2(p_lq)^2 - 4b_2m_K^2(p_lq)^2 + 4g_3m_K^2(p_lq)^2 \\
& - 2a_2m_l^2(p_lq)^2 - 2c_2m_l^2(p_lq)^2 + 4c_3m_l^2(p_lq)^2 + 4e_3m_l^2(p_lq)^2 \\
& - 4a_2(p_lq)^3 + 4c_3(p_lq)^3 - 2a_{11}(p_lq)(ppi) - 4b_{11}(p_lq)(ppi) \\
& + 4J_{12}(p_lq)(ppi) - 8a_2(p_lq)^2(ppi) - 8b_2(p_lq)^2(ppi) + 4b_3(p_lq)^2(ppi) \\
& - 8c_2(p_lq)^2(ppi) + 8d_3(p_lq)^2(ppi) + 8J_1(p_lq)^2(ppi) - 2a_{11}(p_lq)(pq) \\
& - 4b_{11}(p_lq)(pq) + 4J_{12}(p_lq)(pq) + 4b_3(p_lq)^2(pq))
\end{aligned}$$

$$C_3 = C_7 = C_{11} = C_{15} = 0$$

## Figure captions

**Fig. 1.** The Feynman diagrams for the  $K^+ \rightarrow \pi^0 l^+ \nu \gamma$  decay at the tree level of SM.

**Fig. 2.** Branching differential distribution over the pion, lepton,  $\gamma$ -quantum momenta and the angle between the lepton and  $\gamma$ -quantum in the  $K$ -meson rest frame for the cases of (a) electron and (b) muon decay channels.

**Fig. 3.**  $\xi$ -dependence of the  $K^+ \rightarrow \pi^0 l^+ \nu \gamma$  branching at the tree level of SM for the (a) electron and (b) muon channels.

**Fig. 4.** The Feynman diagrams contributing to the imaginary parts of formfactors (10) at the one-loop level of SM.

**Fig. 5.**  $\xi$ -odd contributions,  $f_{odd}$ , to the branching differential distribution for the (a) electron and (b) muon decay channels.

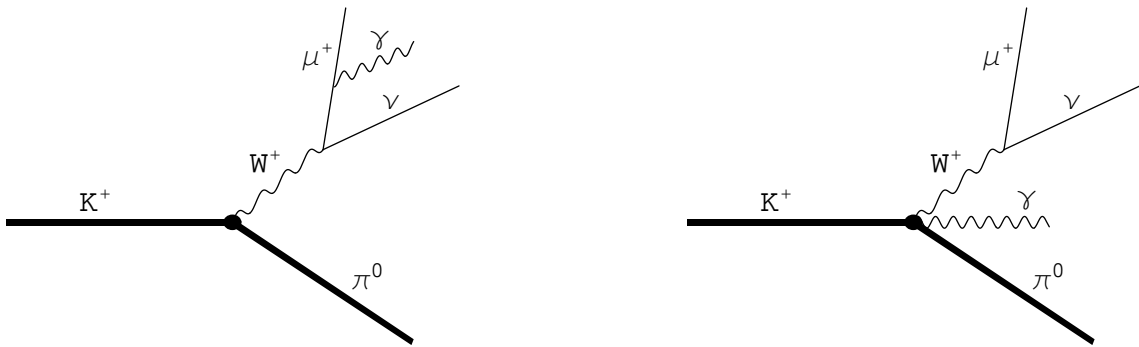


**Fig. 1**

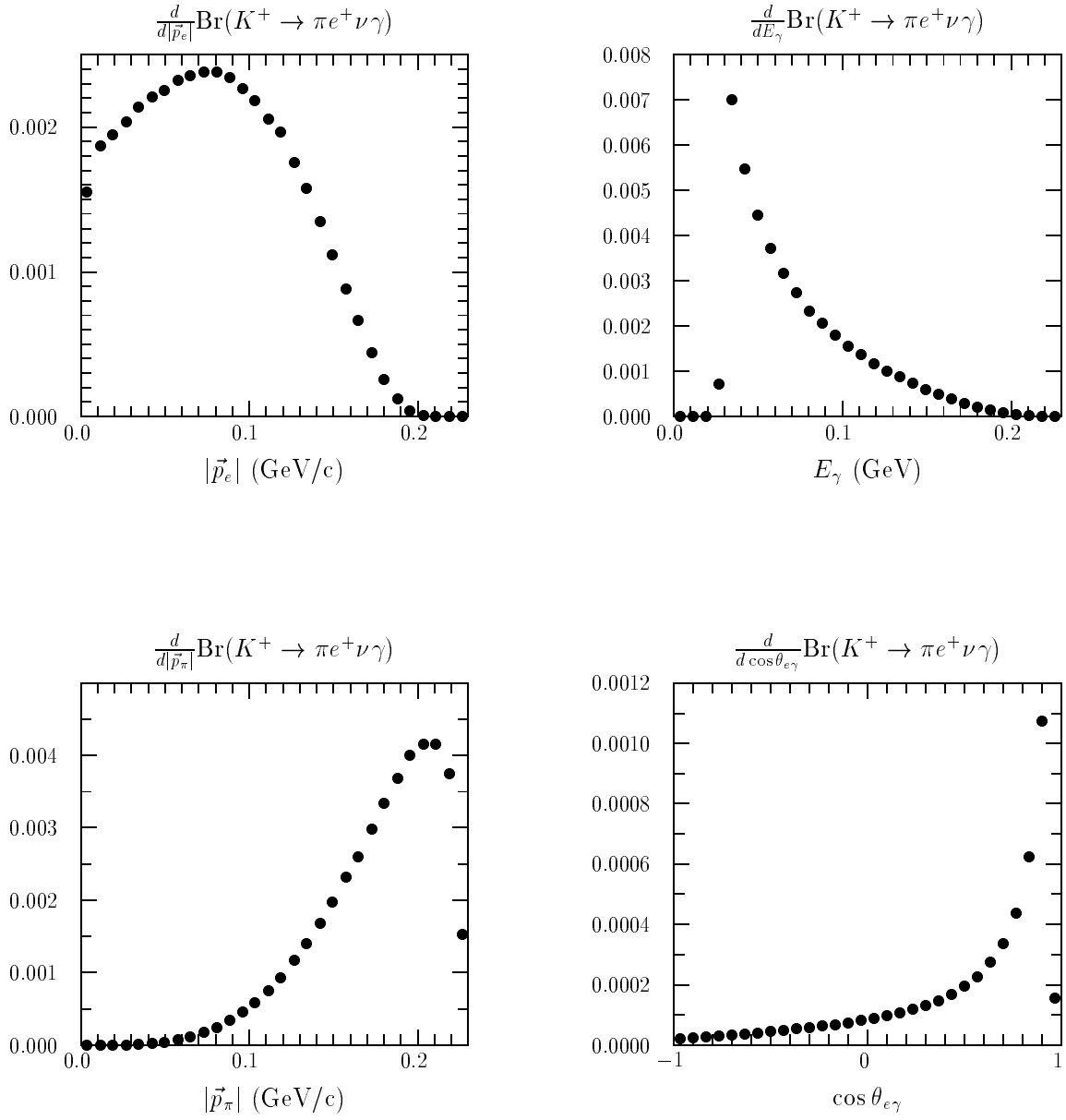


Fig. 2a

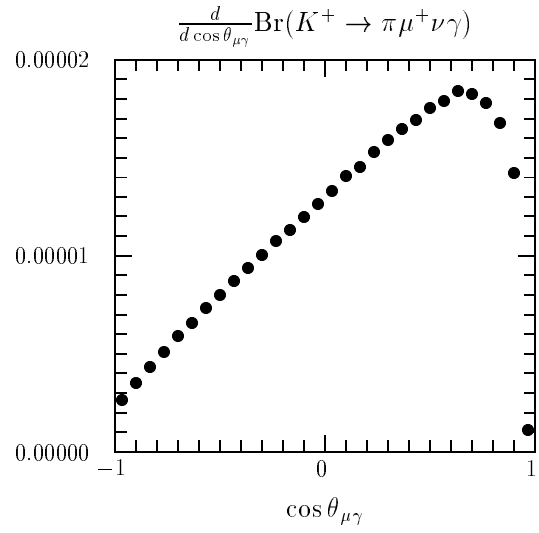
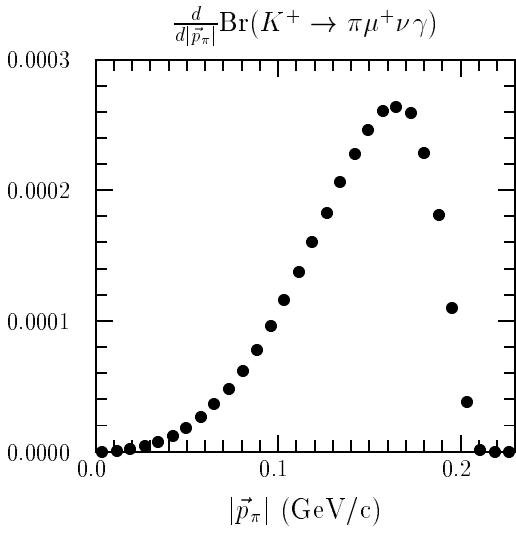
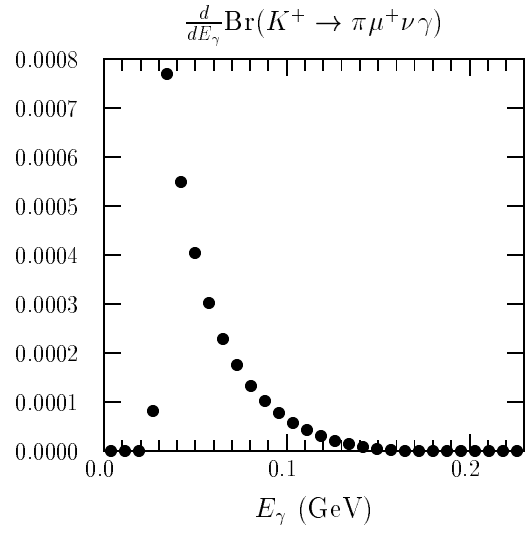
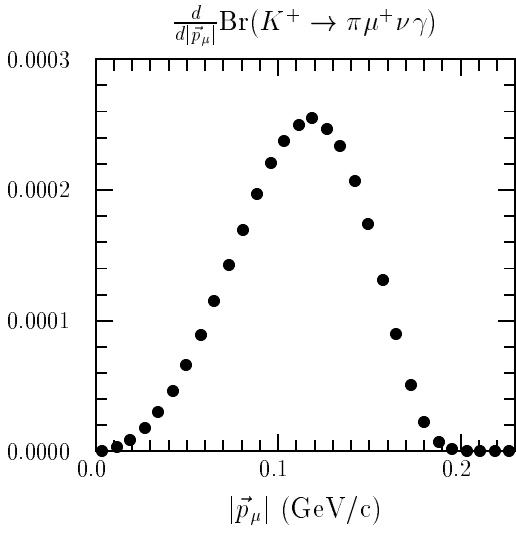


Fig. 2b

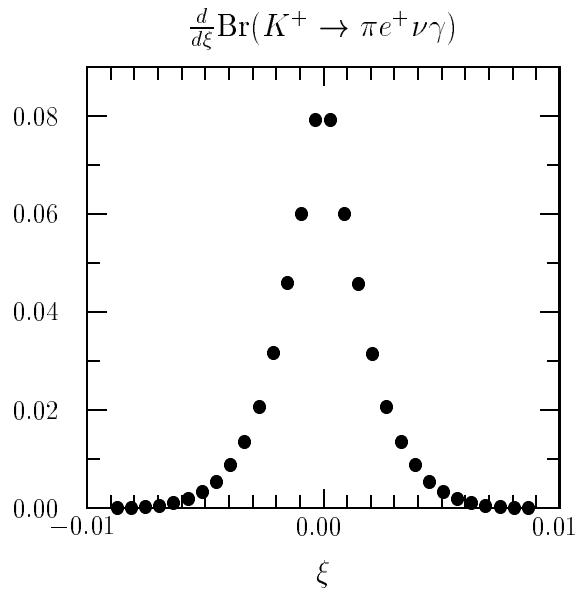


Fig. 3a

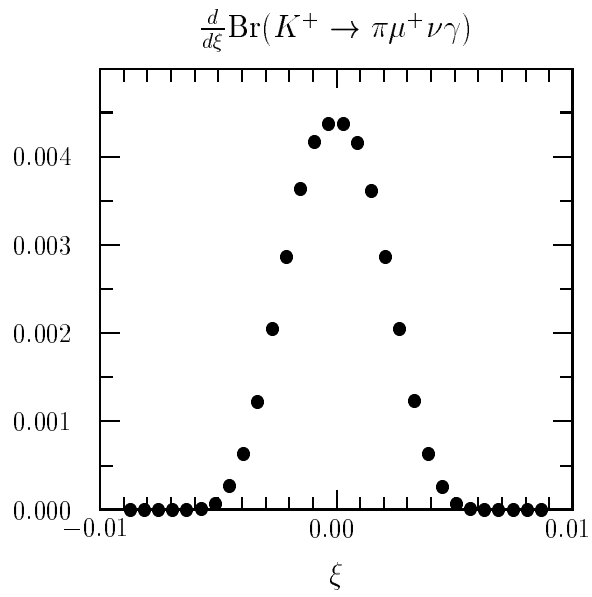
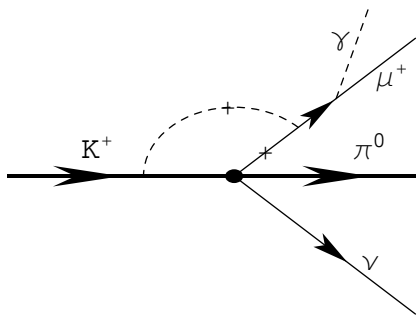
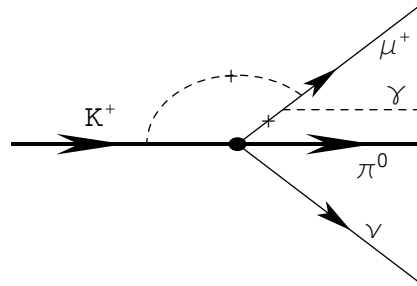


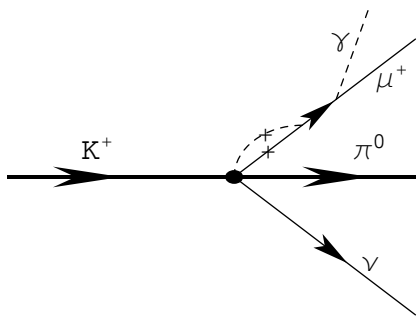
Fig. 3b



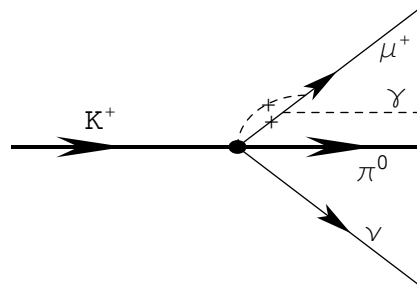
(a)



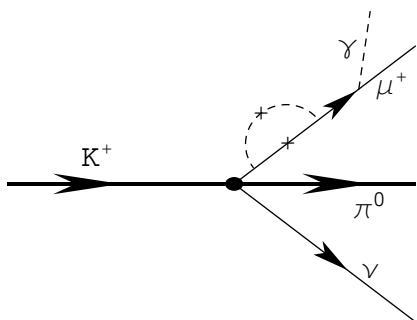
(b)



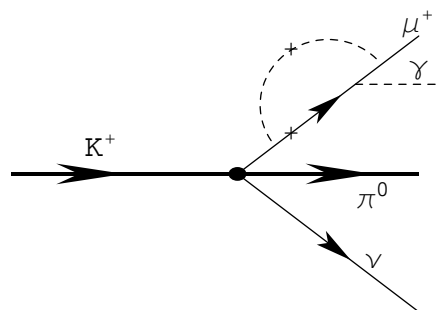
(c)



(d)



(e)



(f)

Fig. 4

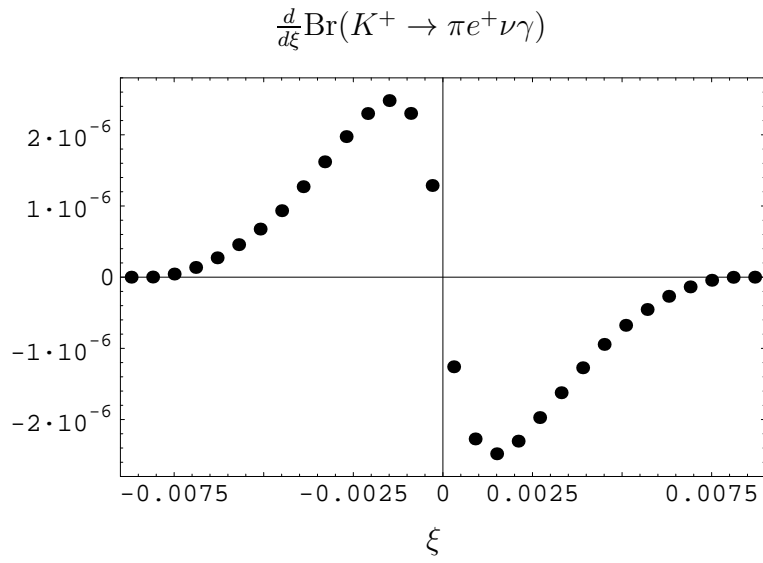


**Fig. 5a**

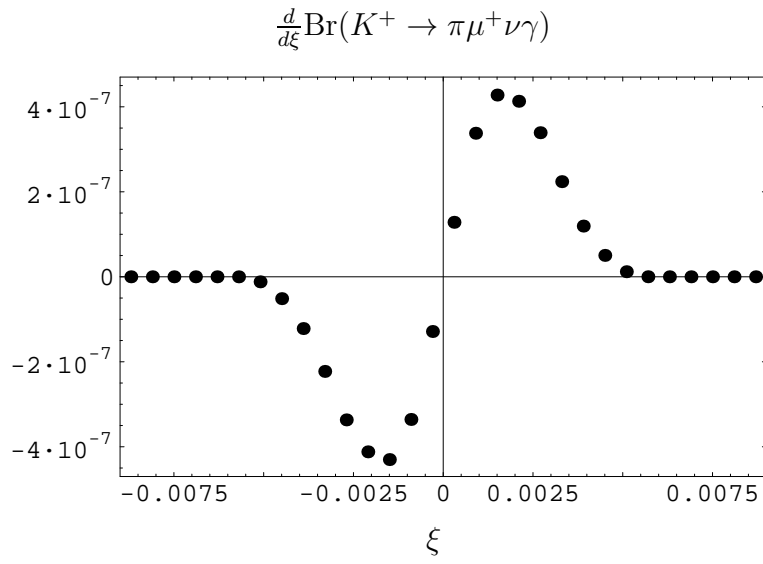


**Fig. 5b**